

# The millimeter-wave bolometric interferometer (MBI)

Gregory S. Tucker<sup>\*a</sup>, Andrei L. Korotkov<sup>a</sup>, Amanda C. Gault<sup>b</sup>, Peter O. Hyland<sup>b</sup>, Siddharth Malu<sup>b</sup>, Peter T. Timbie<sup>b</sup>, Emory F. Bunn<sup>c</sup>, Brian G. Keating<sup>d</sup>, Evan Bierman<sup>d</sup>, Cr  idhe O’Sullivan<sup>e</sup> Peter A. R. Ade<sup>f</sup>, Lucio Piccirillo<sup>g</sup>

<sup>a</sup>Dept. of Physics, Box 1843, Brown Univ., 182 Hope St., Providence, RI, USA 02912;

<sup>b</sup>Dept. of Physics, Univ. of Wisconsin, 1150 University Ave., Madison, WI USA 53706;

<sup>c</sup>Dept. of Physics, Univ. of Richmond, Richmond, VA USA 23173;

<sup>d</sup>Dept. of Physics, Univ. of California, 9500 Gilman Drive, La Jolla, CA USA 92093;

<sup>e</sup>Dept. of Exp. Physics, National Univ. of Ireland, Maynooth, Co. Kildare, Ireland;

<sup>f</sup>Dept. of Physics and Astronomy, Univ. of Wales, Queen’s Building 5 The Parade, Cardiff, CF24 3YB United Kingdom;

<sup>g</sup>The School of Physics and Astronomy, The University of Manchester, Oxford Road, Manchester, M13 9PL, UK

## ABSTRACT

We report on the design and tests of a prototype of the Millimeter-wave Bolometric Interferometer (MBI). MBI is designed to make sensitive measurements of the polarization of the cosmic microwave background (CMB). It combines the differencing capabilities of an interferometer with the high sensitivity of bolometers at millimeter wavelengths. The prototype, which we call MBI-4, views the sky directly through four corrugated horn antennas. MBI ultimately will have  $\sim 1000$  antennas. These antennas have low sidelobes and nearly symmetric beam patterns, so spurious instrumental polarization from reflective optics is avoided. The MBI-4 optical band is defined by filters with a central frequency of 90 GHz. The set of baselines, determined by placement of the four antennas, results in sensitivity to CMB polarization fluctuations over the multipole range  $\ell = 150 - 270$ . The signals are combined with a Fizeau beam combiner and interference fringes are detected by an array of spider-web bolometers. In order to separate the visibility signals from the total power detected by each bolometer, the phase of the signal from each antenna is modulated by a ferrite-based waveguide phase shifter. Initial tests and observations have been made at Pine Bluff Observatory (PBO) outside Madison, WI.

**Keywords:** cosmic microwave background, polarization, interferometer, bolometer

## 1. INTRODUCTION

We have built a prototype version of an instrument called the Millimeter-wave Bolometric Interferometer (MBI) for observing faint astrophysical sources. We have started test observations with the prototype (MBI-4) from Pine Bluff Observatory (PBO) near Madison, WI. The main scientific goal of MBI is to search for primordial B-mode polarization in the cosmic microwave background (CMB).

A significant challenge in CMB polarization measurements is separation of the very weak pseudoscalar B component from the much stronger scalar E component.<sup>1,2</sup> The two types of polarization modes probe different physical phenomena; in particular, ordinary density (scalar) perturbations produce only E-type polarization (to linear order). As a result, the B component is predicted to be smaller than E by an order of magnitude or more over all angular scales. However, the very fact that density perturbations do not produce B-type polarization makes detection of the B component more valuable: the B channel is a clean probe of other types of perturbations.

The most exciting prospect is the use of B modes to detect primordial gravitational waves (tensor perturbations) produced during an inflationary epoch. If this tensor B component is detected, we will have a direct probe of the Universe at far earlier times than any other method can provide. The other dominant source of B-type

---

\*Gregory\_Tucker@brown.edu; Telephone: 1 401 863-1441

polarization in the CMB is expected to be gravitational lensing of E modes by large-scale structure. These two predicted sources of B modes probe very different epochs: the tensor contribution is imprinted on the CMB at the time of last scattering but is a relic of the extremely early Universe; the lensing contribution is produced at much later times. The lensing signal peaks at relatively small angular scales ( $< 1^\circ$ ), while the tensor signal (if it exists) is strongest on large scales.

## 2. EXPERIMENTAL APPROACH

### 2.1 Why MBI?

MBI combines the differencing capabilities of an interferometer with the high sensitivity of bolometers to yield new capabilities that would be difficult or impossible to achieve using more traditional techniques. Cooled bolometers are the highest-sensitivity broadband detectors at millimeter and sub-millimeter wavelengths; they can achieve the fundamental noise limit imposed by photon noise from the CMB itself. There are a number of advantages achieved in combining the two technologies.

Unlike a single-dish imaging telescope, an interferometer instantaneously performs a differential measurement: the effective “beam pattern” of each individual baseline is a set of fringes that sample the sky with positive and negative weights. This differencing removes the need for mechanical chopping or rapid scanning. Only correlated signals are detected, so the interferometer has reduced sensitivity to changes in the total power signal absorbed by the detectors.<sup>3</sup> Thus the signal from an interferometer is significantly less affected by the atmosphere.<sup>4,5</sup>

Another advantage of an interferometer is in the control of systematic effects. For example, when using a traditional telescope in conjunction with a focal-plane array to measure CMB anisotropy, there are several design issues. The telescope provides angular resolution, but to get sensitivity a large number of detectors must be placed in the focal plane. Obtaining a low cross-polarization, large field-of-view optical design for such a system is challenging. An alternate approach is to observe the sky directly with corrugated horn antennas. This has several advantages. The optical design is simple and clean. A large number of corrugated horns antennas, not limited in number by a telescope design, can be used to obtain sensitivity. The cost of this approach is the loss of angular resolution unless extremely large number of corrugated horn antennas are used. MBI takes the second approach, but adds interferometry between corrugated horn antennas to recover some of the angular resolution lost by dispensing with a telescope. Bunn has carried out a detailed analysis of systematic effects in interferometers;<sup>6</sup> a similar analysis has been undertaken for imaging systems.<sup>7</sup>

A traditional radio interferometer correlates signals between pairs of antennas to form visibilities for each baseline. Each visibility is a measurement of a single Fourier mode on the sky and corresponds to a single multipole in the CMB power spectrum. Using aperture synthesis these visibilities can be combined to form an image. However, such an interferometer is not sensitive to angular scales larger than the instantaneous field-of-view. However, as explained below, because MBI is an adding interferometer it can obtain this large angular scale (low multipole) information because it measures the visibilities from each of its baselines and simultaneously forms an image of the sky.

### 2.2 The Adding Interferometer

In a simple two-element radio interferometer, signals from two telescopes aimed at the same point in the sky are correlated (multiplied) so that the sky temperature is sampled with an interference pattern with a single spatial frequency. The output of such an interferometer at a single wavelength is the visibility,  $V(\vec{u}) \propto \int G(\hat{x}) \Delta T(\hat{x}) e^{i2\pi\vec{u}\cdot\hat{x}} d\hat{x}$ , where  $\hat{x}$  is a unit 3-vector in the direction of a point on the sky,  $G(\hat{x})$  is the beam pattern of each antenna (assumed to be identical), and  $\Delta T(\hat{x})$  is the map of temperature fluctuations on the sky we are trying to measure. ( $\Delta T(\hat{x}) \propto E_0^2$ .) The vector  $\vec{u}$  has length  $B/\lambda$ , the baseline length in wavelength units, and is oriented along the baseline. With more telescopes these same correlations are performed along each baseline. To recover the full phase information, complex correlators are used to measure simultaneously both the in-phase and quadrature phase components of the visibility.

In interferometers that use incoherent detectors, such as MBI, the electric field wavefronts from two telescopes are added and then squared in a detector as shown in Fig. 1 — an “adding” interferometer as opposed to a “multiplying” interferometer.<sup>8</sup> The result is a constant term proportional to the intensity plus an interference

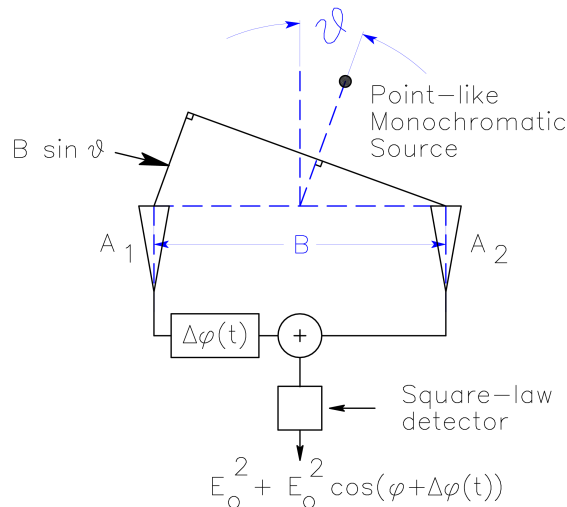


Figure 1. Adding interferometer. At antenna  $A_2$  the electric field is  $E_0$ , and at  $A_1$  it is  $E_0 e^{i\phi}$ , where  $\phi = kB \sin \theta$  and  $k = 2\pi/\lambda$ .  $B$  is the length of the baseline, and  $\alpha$  is the angle of the source with respect to the symmetry axis of the baseline, as shown. (For simplicity consider only one wavelength,  $\lambda$ , and ignore time dependent factors.) In a multiplying interferometer the in-phase output of the correlator is proportional to  $E_0^2 \cos \phi$ . For the adding interferometer, the output is proportional to  $E_0^2 + E_0^2 \cos(\phi + \Delta\phi(t))$ . The desired signal is recovered by introducing a time dependent phase modulation  $\Delta\phi(t)$  in one arm of the interferometer.

term. The constant term is an offset that is removed by phase modulating one of the signals. Phase-sensitive detection at the modulation frequency recovers the interference term and reduces susceptibility to low-frequency drifts ( $1/f$  noise) in the bolometer and readout electronics. The adding interferometer recovers the same visibility as a multiplying interferometer.

An interferometer measures the Stokes parameters directly, without differencing the signal from separate detectors. An interferometer correlates the components of the electric field captured by each antenna with the components from all of the other antennas. On the baseline formed by two antennas, 1 and 2, the interferometer's correlators measure  $\langle E_{1x} E_{2x} \rangle$ ,  $\langle E_{1y} E_{2y} \rangle$ ,  $\langle E_{1x} E_{2y} \rangle$ , and  $\langle E_{1y} E_{2x} \rangle$ . The first two are used to determine  $I$  and the latter two measure  $U$ . Rotating the instrument allows a measurement of  $Q$ . Stokes  $V$  can be recovered in a similar manner but is expected to be zero for the CMB; we do not plan on measuring it.

The sensitivity of a receiver to broadband signals increases as the square root of the bandwidth. For interferometers, the bandwidth restricts the angular range,  $\theta$ , over which fringes are detected.<sup>9,10</sup> If we assume the path lengths for a source at the center of the FOV are equal, then the path length difference for a source at an angle  $\theta$  from the center along the baseline axis is  $\theta B$ . If this path length difference is small compared to the coherence length of the light,  $\lambda^2/\Delta\lambda$ , then the fringe contrast is not affected. Thus the FOV is determined by  $\theta_{\text{FOV}} \leq (\lambda/\Delta\lambda)(\lambda/B)$ . This equation indicates that for angles of the order of the product of the spectral resolution times the angular resolution, the fringe smearing is important. This relation imposes restrictions on the ratio between the maximum baseline achievable by the interferometer and the spectral bandwidth of the receiver. For MBI the bandwidth is 15%, which sets the maximum baseline to about six times the diameter of each antenna.

### 2.3 Sensitivity

In this section we estimate the expected sensitivity of MBI. We show that the sensitivity of an interferometer is comparable to that of a filled-dish telescope collecting the same number of modes from the sky. Since MBI operates as both an interferometer and imager, it useful to consider three cases: Conventional Imaging System, MBI Interferometer and MBI Imaging Mode.

### 2.3.1 Case 1: Conventional Imaging System

Assume we collect radiation from the sky onto an array of  $N$  single-mode corrugated horn antennas. These horns could be at the focus of a telescope or could view the sky directly. Let each horn couple to two polarizations. The optical throughput is  $A\Omega = N\lambda^2$ , where  $N$  is the number of spatial modes (which equals the number of horns). Following each horn, labeled  $i$ , the electric field is split by an OMT into orthogonal components  $E_{ix}$  and  $E_{iy}$ . Each is detected by a separate bolometer. The optical efficiency from telescope entrance through detector absorption is  $\eta$ . The optical signal occupies a bandwidth  $\Delta\nu$ . The intensity of the CMB electric field signal that enters a horn labeled  $i$  is proportional to  $|E_i|^2$ . For simplicity assume the bolometer noise is background-limited either by the CMB or by emission from the optics. Also assume a low background (balloon and space), where the photon occupation number is much less than one,  $BLIP \sim \sqrt{\text{optical loading}}$ . The sensitivity to CMB temperature fluctuations in each detected polarization for each horn (in units of  $K\sqrt{s}$ ) is then

$$\Delta T_{1-\text{dtr}} = \frac{BLIP_{1-\text{dtr}}}{\sqrt{2}(dP/dT)},$$

where  $dP/dT$  is the derivative with respect to temperature of the CMB power absorbed by the bolometer, evaluated at  $T = 2.7$  K.  $P = \eta B_\nu \lambda^2 \Delta\nu$  where  $B_\nu$  is the Planck brightness. The sensitivity of an imager with  $N$  of these horns is

$$\Delta T_{\text{imager}} = \Delta T_{1-\text{dtr}}/\sqrt{2N}.$$

### 2.3.2 Case 2: MBI Interferometer Mode

Assume the interferometer is a two-dimensional close-packed array of  $N$  horn antennas that each collects one spatial mode and two polarizations directly from the sky. This system has the same throughput and number of modes  $N$  as the imager above. As above, following each horn, labeled  $i$ , the electric field is split by an OMT into orthogonal components  $E_{ix}$  and  $E_{iy}$ . (Equivalently, the field could be split into right and left circular polarization modes.) Electronic phase modulators switch the phase of each signal  $\pm 90^\circ$  in a sequence described below. After  $\pm 45^\circ$  twists these signals pass through small horn antennas that illuminate the primary mirror of a small telescope — a Fizeau beam combiner.<sup>11</sup> The twists are required on all of the signals to bring them into the same polarization state in the focal plane. The entering beams are all parallel to the telescope axis, so the electric field amplitudes from all the horns overlap at the center of the combiner's focal plane. The detectors square the sum of these amplitudes and produce interference fringes that are measured by an array of cold bolometers that cover the focal plane. For simplicity assume uniform illumination of the pixels in the bolometer array, which has  $N_{\text{bol}} = 4N$  bolometers. (For a close-packed array of  $N$  horns, pairs of horns at the largest separations will be about  $\sqrt{N}$  horn diameters apart and will create approximately  $\sqrt{N}$  fringes in the focal plane. To Nyquist sample these fringes we require  $2\sqrt{N}$  pixels in each dimension or  $4N$  pixels in two dimensions.)

For each pair of horns we detect fringes in the focal plane that correspond to a visibility determined by the separation and orientation of that particular baseline. The visibility is proportional to the product of the amplitudes of the electric fields transmitted by the horns (*i.e.*,  $E_{i\alpha}E_{j\beta}^*$  where  $i$  and  $j$  label the horns and  $\alpha$  and  $\beta$  label the polarizations,  $x$  and  $y$ ). Accounting for polarization, there are  $2N(2N - 2)$  “cross-terms” where  $i \neq j$ . These terms represent the pairwise interference between different antennas and can be combined to form the  $2N(2N - 2)/2$  visibilities expected in an  $N$ -element interferometer detecting 2 polarizations.

The fraction of a particular visibility signal that reaches a single bolometer is proportional to  $E_{ix}E_{jy}^*/4N$ , decreasing the S/N on each bolometer by a factor of  $4N$ . But there are  $4N$  bolometers that measure this visibility, improving the S/N by a factor of  $\sqrt{4N}$ . Assuming the same optical efficiency,  $\eta$ , as above, the optical loading on each bolometer is now a factor of  $N/4N = 1/4$  the loading of case 1; the noise of each bolometer is a factor of 2 smaller. So the sensitivity to a single visibility compared to the measurement of total power in Case 1 is

$$\Delta T_{\text{Interferometer}} = \sqrt{N}\Delta T_{1-\text{dtr}}.$$

The noise in each visibility is  $\sqrt{N}$  larger than the noise per detector in the imaging. However, the interferometer measures  $\sim N^2$  independent numbers (visibilities), as opposed to  $N$  independent numbers in the imaging case. The overall sensitivities are, therefore, comparable.

In order to separate these interference terms from each other we modulate the phase of the antenna signals in a sequence. By differencing the detector outputs that appear during each phase state, we can isolate the various visibilities. This scheme amounts to a kind of time-domain multiplexing of the signals from the various baselines onto each detector.

We have performed a more formal analysis of this system following the approach developed by Zmuidzinas (2003).<sup>12</sup> He shows how to compare the sensitivity of a filled-dish imaging system with interferometers that employ various kinds of beam combination. For simplicity, we assumed a one-dimensional, close-packed interferometer array with a Butler combiner (the waveguide equivalent of a Fizeau combiner) and compared it with a one-dimensional filled dish; the sensitivity of the two systems is comparable.

### 2.3.3 Case 3: MBI Imaging Mode

Besides operating as an interferometer, which measures visibilities for the various MBI baselines, MBI simultaneously functions as an imaging instrument. Using the same arrangement as in Case 2, we control the phase modulators in such a way that an image appears on the focal plane. For example, by setting each phase shifter for the  $x$  components of each OMT to  $0^\circ$ , and turning the  $y$  component phase shifters off (closed) we add together in the focal plane the fields  $E_{ix}$  from each of the horns. The superposition of fringe patterns created by the many baseline pairs forms a crude image in the focal plane with angular resolution determined by the longest horn baselines. In the limit of an infinite number of horns the MBI aperture is open, the image improves, and MBI becomes an imaging telescope. Similarly, an image of the sky can be formed using just the  $y$  components of the electric field. By rapidly switching between these two phase states we can compare  $x$  and  $y$  polarization images of the sky and thus measure Stokes  $Q$ . Alternatively the phase fronts can be controlled to form an image of the sky that is proportional to  $E_x E_y$ , or Stokes  $U$ . By simultaneously switching all the  $x$  phase modulators with respect to the  $y$  modulators the sign of the desired  $U$  signal is inverted and can be separated from offsets and other instrumental effects. In all of these cases the phase modulators are switched in unison so that the signals from all  $N$  horns add together, improving the S/N by a full factor of  $N$ . The sensitivity of the entire array of  $N$  horns in this case is

$$\Delta T_{\text{MBI-Imager}} = \frac{\Delta T_{1-\text{dtr}}}{\sqrt{N}}.$$

This is comparable to the sensitivity of an imaging system collecting  $N$  modes. Although the signal from each antenna in MBI is split among detectors in the focal plane, we recover the same sensitivity as a filled-dish by combining the signals from these detectors.

For simplicity, these sensitivity comparisons have assumed background-limited detectors in a low-background environment. We are also developing a noise model for MBI in the higher backgrounds in which it is being tested.

## 3. INSTRUMENT

The basic input unit (IU) of MBI is shown in Fig. 2. The beam width of the MBI input corrugated horn antenna is  $\sim 8^\circ$ . The signals from an IU and between IUs are interfered using a so-called Fizeau beam combiner as shown in Fig. 3. The Fizeau combiner acts as an image-plane correlator or adding interferometer. In MBI, the Fizeau combiner is essentially a Cassegrain telescope. All signals from the IUs illuminate the primary mirror, and the light is correlated or interfered on an array of 16 bolometers at the focal plane behind the primary mirror.

### 3.1 Phase Modulators

In order to separate the interference (visibility) signals from the total power signal detected by each bolometer, the phase of the signal from each antenna must be modulated. We modulate the phase between  $-90^\circ$  and  $+90^\circ$  in a stepped sequence, similar to that of a Walsh function, so that redundant visibilities are measured simultaneously.

For MBI we are using ferrite devices in waveguide; these are a modification of the Faraday rotation modulators that were used in BiCEP.<sup>13</sup> We switch the modulators at  $\sim 3$  Hz. The loss in the phase shifter is  $< 1$  dB. The phase shifters dissipate negligible power,  $\sim 1$  mW each. Also, the differential loss between the two phase states must be small. Differential loss will produce an “offset” signal after demodulation of the detector signal. Fig. 4 indicates that this differential loss is small.

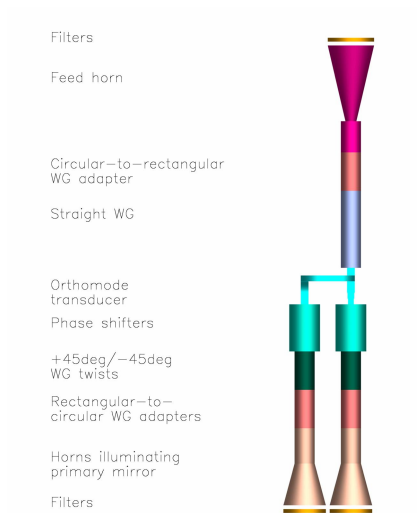


Figure 2. Input unit (IU) of the MBI interferometer. All optical components are housed in a helium cryostat. With the exception of the window and input filters all of the optical components are at 4 K. Light enters from the top and passes through three sets of filters at 300 K, 77 K and 4 K before entering the horn antenna. The two polarizations are separated using an ortho-mode transducer (OMT). The two polarizations are rotated in waveguide (WG) so that the two polarization vectors are aligned. A  $\pm 90^\circ$  phase modulation is introduced in one of the arms and the two signals are directed at the Fizeau combiner. The interference of signals from different IUs results in an interferometer. In MBI-4 there are no OMTs, so each horn antenna is sensitive to only a single polarization.

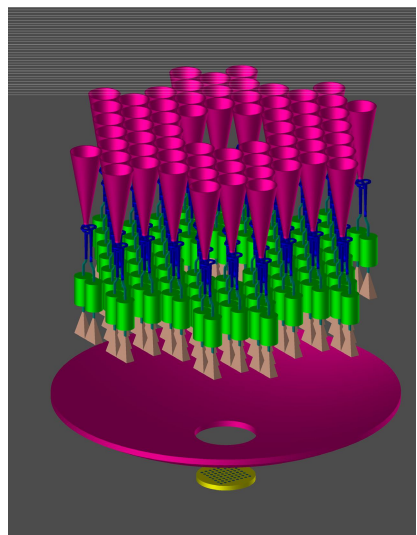


Figure 3. A three-dimensional view of 64 IUs arranged in a close-packed array illuminating a Fizeau combiner. The detector array sits behind the primary mirror of the beam combiner. Note that the distances between the IUs, primary mirror and detector array are not to scale and the secondary mirror is partially obscured by the horn antennas. MBI-4 uses a similar beam combiner with a sparse array of four, single polarization, horn antennas.

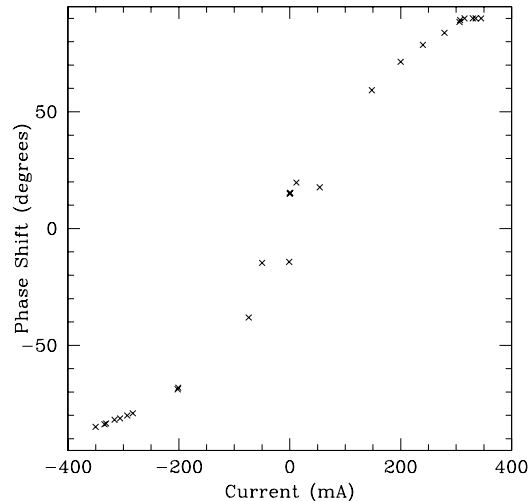


Figure 4. Measured phase shift produced by one of the four Faraday rotation phase modulators used in MBI as a function of the current driven through the modulator's superconducting magnetic coil. The modulator switches the phase of the RF signal between  $\pm 90$  degrees when the drive current is switched between  $\pm 300$  mA. The ferrite material is operated near saturation, so the phase is insensitive to small variations in drive current and to hysteresis effects. Hysteresis is visible in the separation between the two curves at currents between  $-50$  mA and  $+50$  mA.

### 3.2 Detectors and Filters

MBI uses 16 traditional spider-web bolometers with NTD germanium thermistors. These bolometers are based on bolometers used for ACBAR.<sup>14</sup> These bolometers are coupled to the focal plane using a close-packed array of horns. Each MBI feed horn views the sky directly through a vacuum window.

### 3.3 Cryogenics

The MBI cryostat holds 17 liters of liquid nitrogen and 25.7 liters of liquid helium. In its operational configuration the liquid helium lasts for 30 hours.

The detectors are cooled by a self-contained "He-10" refrigerator manufactured by Chase Cryogenic Research. A  $^3\text{He}$  "ultrahead" is cooled to below 260 mK using a self-contained charcoal-pumped  $^3\text{He}$  condenser, which is cooled by a self-contained charcoal-pumped  $^4\text{He}$  pot. In its operational configuration the  $^3\text{He}$  refrigerator remains cold for more than 24 hours. Cycling the refrigerator takes about one hour.

### 3.4 Pointing platform

The MBI pointing platform consists of a fully-steerable altitude-azimuth mount. This mount is based on the one developed for the COMPASS experiment.<sup>15</sup> In addition, the entire cryostat can be rotated around the optical ("theta") axis. Tracking of the sky occurs under computer control using feedback from 17-bit absolute optical encoders on each of the three axes - altitude, azimuth and theta. Absolute pointing is established using a bore-sited optical telescope.

## 4. RESULTS

This year we started test observations with MBI at Pine Bluff Observatory, near the University of Wisconsin, Madison. A photo of MBI at PBO is shown in Fig. 5. As part of testing MBI scanned a narrow band source located in the far field; the fringes resulting from one such scan are shown in Fig. 6. The relative positions of the input corrugated horn antennas is shown in Fig. 7. We are analyzing the data from these test observations and are comparing the observed fringe patterns with a physical optics model which we have developed. We are particularly interested in determining the far sidelobe response of the instrument.



Figure 5. The MBI instrument observing the zenith at Pine Bluff Observatory in the winter of 2008. The octagonal structure above the cryostat is a ground shield.

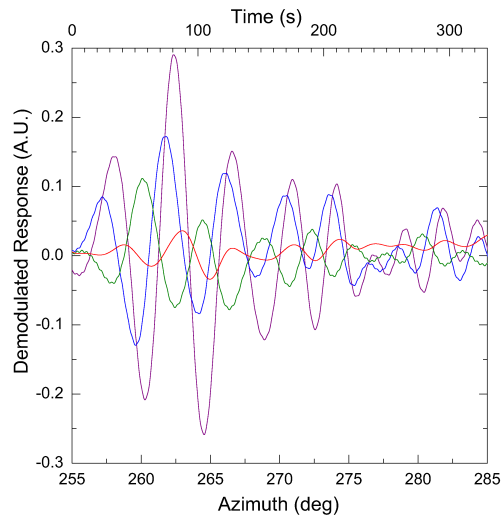


Figure 6. Signals from four bolometers as MBI scanned in azimuth a far-field narrow band source — a Gunn oscillator. The oscillator was located on a 15 m tall tower. During the scan, antennas 1 and 4 were open and the phase in antenna 1 was modulated using the phase shifter. The observed fringe patterns are in accordance with what we expect given the different locations of the bolometers in the focal plane. At the time of this test 12 of 16 bolometers were operational. The signals from only four bolometers are shown for clarity.

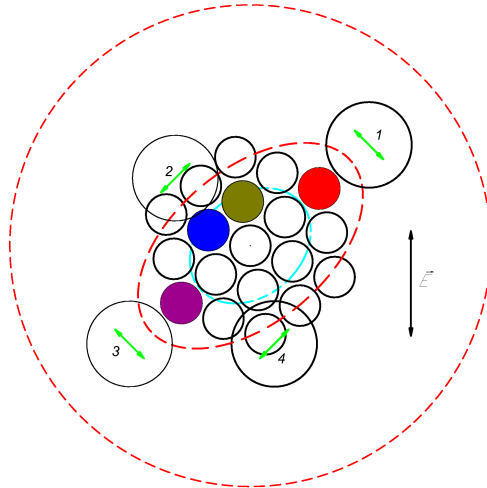


Figure 7. The relative positions of the input horn antennas (labeled 1 through 4) and of the bolometers in the focal plane in MBI-4 are shown. The polarization selected by each input horn antenna is indicated. The dashed red (dark) lines indicate the outline of the Fizeau combiner primary mirror, and the dashed cyan (light) line indicates the outline of the secondary. As drawn here, the relative positions of components and scan in azimuth correspond to the measurement shown in Fig 6. The horn apertures are approximately 5 cm in diameter.

## 5. CONCLUSION

We are designing a MBI module with 64 antennas that could be scaled to wavelengths between 1 cm and 1 mm. An instrument formed by several of these modules would have sensitivity for measuring CMB B mode polarization and would survey the sky with identical window functions at each wavelength. We have completed a NASA mission concept study for a spaced-based version of MBI called the Einstein Polarization Interferometer for Cosmology (EPIC).<sup>16</sup>

## ACKNOWLEDGMENTS

This work was supported by NASA grants NAG5-12758, NNX07AG82G, the Rhode Island Space Grant and the Wisconsin Space Grant.

## REFERENCES

- [1] Zaldarriaga, M. and Seljak, U., “All-sky analysis of polarization in the microwave background,” *PRD* **55**, 1830–1840 (Feb. 1997).
- [2] Kamionkowski, M., Kosowsky, A., and Stebbins, A., “Statistics of cosmic microwave background polarization,” *PRD* **55**, 7368–7388 (June 1997).
- [3] White, M., Carlstrom, J. E., Dragovan, M., and Holzzapfel, W. L., “Interferometric Observation of Cosmic Microwave Background Anisotropies,” *ApJ* **514**, 12–24 (Mar. 1999).
- [4] Church, S. E., “Predicting residual levels of atmospheric sky noise in ground based observations of the cosmic microwave background radiation,” *MNRAS* **272**, 551–569 (Feb. 1995).
- [5] Lay, O. P. and Halverson, N. W., “The Impact of Atmospheric Fluctuations on Degree-Scale Imaging of the Cosmic Microwave Background,” *ApJ* **543**, 787–798 (Nov. 2000).
- [6] Bunn, E. F., “Systematic errors in cosmic microwave background interferometry,” *PRD* **75**, 083517–+ (Apr. 2007).
- [7] Hu, W., Hedman, M. M., and Zaldarriaga, M., “Benchmark parameters for CMB polarization experiments,” *PRD* **67**, 043004–+ (Feb. 2003).
- [8] Rohlfs, K. and Wilson, T. L., [*Tools of Radio Astronomy*], Springer, New York (1996 (second edition)).

- [9] A. R. Thompson, J. M. M. and Swenson, G. W., [*Interferometry and Synthesis in Radio Astronomy*], Krieger, Florida (1998).
- [10] Böker, T. and Allen, R. J., “Imaging and Nulling with the SPACE INTERFEROMETER MISSION,” *ApJS* **125**, 123–142 (Nov. 1999).
- [11] Fizeau, H. *Comptes Rendus de l’Académie des Sciences* **66**, 932 (1868).
- [12] Zmuidzinas, J., “Cramér-Rao sensitivity limits for astronomical instruments: implications for interferometer design,” *Journal of the Optical Society of America A* **20**, 218–233 (Feb. 2003).
- [13] Yoon, K. W., Ade, P. A. R., Barkats, D., Battle, J. O., Bierman, E. M., Bock, J. J., Brevik, J. A., Chiang, H. C., Crites, A., Dowell, C. D., Duband, L., Griffin, G. S., Hivon, E. F., Holzzapfel, W. L., Hristov, V. V., Keating, B. G., Kovac, J. M., Kuo, C. L., Lange, A. E., Leitch, E. M., Mason, P. V., Nguyen, H. T., Ponthieu, N., Takahashi, Y. D., Renbarger, T., Weintraub, L. C., and Woolsey, D., “The Robinson Gravitational Wave Background Telescope (BICEP): a bolometric large angular scale CMB polarimeter,” in [*Millimeter and Submillimeter Detectors and Instrumentation for Astronomy III. Edited by Zmuidzinas, Jonas; Holland, Wayne S.; Withington, Stafford; Duncan, William D.. Proceedings of the SPIE, Volume 6275, pp. 62751K (2006).*], Presented at the Society of Photo-Optical Instrumentation Engineers (SPIE) Conference **6275** (July 2006).
- [14] Runyan, M. C., Ade, P. A. R., Bhatia, R. S., Bock, J. J., Daub, M. D., Goldstein, J. H., Haynes, C. V., Holzzapfel, W. L., Kuo, C. L., Lange, A. E., Leong, J., Lueker, M., Newcomb, M., Peterson, J. B., Reichardt, C., Ruhl, J., Sirbi, G., Torbet, E., Tucker, C., Turner, A. D., and Woolsey, D., “ACBAR: The Arcminute Cosmology Bolometer Array Receiver,” *ApJS* **149**, 265–287 (Dec. 2003).
- [15] Farese, P. C., Dall’Oglio, G., Gundersen, J. O., Keating, B. G., Klawikowski, S., Knox, L., Levy, A., Lubin, P. M., O’Dell, C. W., Peel, A., Piccirillo, L., Ruhl, J., and Timbie, P. T., “COMPASS: An Upper Limit on Cosmic Microwave Background Polarization at an Angular Scale of 20’,” *ApJ* **610**, 625–634 (Aug. 2004).
- [16] Timbie, P. T., Tucker, G. S., Ade, P. A. R., Ali, S., Bierman, E., Bunn, E. F., Calderon, C., Gault, A. C., Hyland, P. O., Keating, B. G., Kim, J., Korotkov, A., Malu, S. S., Mauskopf, P., Murphy, J. A., O’Sullivan, C., Piccirillo, L., and Wandelt, B. D., “The Einstein polarization interferometer for cosmology (EPIC) and the millimeter-wave bolometric interferometer (MBI),” *New Astronomy Review* **50**, 999–1008 (Dec. 2006).